International Journal of Modern Physics C, Vol. 12, No. 3 (2001) 421–436

GROUND-STATES OF TWO DIRECTED POLYMERS

V. T. PETÄJÄ and M. J. ALAVA
Helsinki University of Technology, Laboratory of Physics
P. O. Box 1100, FIN-02015 HUT, Finland

H. RIEGER
Theoretische Physik, Universität des Saarlandes, 66041 Saarbrücken, Germany
E-mail: rieger@lusi.uni-sb.de

Received 2 May 2001
Revised 9 May 2001

Joint ground states of two directed polymers in a random medium are investigated. Using exact min-cost flow optimization, the true two-line ground-state is compared with the single line ground state plus its first excited state with "worst-possible" initial conditions, where the two lines start next to each other. It is found that these two-line configurations are (for almost all disorder configurations) distinct implying that the true two-line ground-state is nonseparable, which means that the two-line ground state cannot be obtained by adding a second line to the first line in the one-line ground state without deforming the first line. The effective interaction energy between the two lines scales with the system size with the scaling exponents 0.39 ± 0.03 and 0.21 ± 0.02 in 2D and 3D, respectively.

Keywords: Directed Polymer; Disorder; Ground States; Roughness; Energy Fluctuations.

1. Introduction

The physics of disordered systems has attracted a lot of attention due to the discovery that free energy of extended objects — lines, surfaces and so on — has singular corrections because of the domination of zero-temperature or ground-state effects.[1] The paradigm of such systems is a directed polymer (DP) in a random medium (DPRM). In this particular example, the object minimizes its energy which is determined by two competing forces: the elastic energy cost of wandering on one hand and the energy gain using energetically favorable pins in the environment on the other hand. The result is super-diffusive behavior, and constrained energy fluctuations. The phase space of the DPRM problem is very rich depending on the nature of the correlations in the disorder and dimensionality. In low enough dimensions, the physics is (at arbitrary temperatures) governed by the so-called zero-temperature fixed point if the noise has weak enough correlations including the uncorrelated case. The case with one transverse dimension becomes exactly solvable

in terms of the roughness and energy fluctuation exponents ζ and θ, respectively, due to a mapping to the Kardar–Parisi–Zhang equation.[2] The values are $\zeta = 2/3$ and $\theta_1 = 1/3$ in $d = 2(= 1 + 1)$ dimensions and fulfill the exponent relation $2\zeta - 1 = \theta$. In the $3(= 2 + 1)$-dimensional case, the roughness exponent is approximately 0.62.

In this paper, we study the problem of two polymers in a joint random medium (TPRM) with mutual interactions[3–8] and focus on the repulsive strong coupling limit, i.e., hard core interaction.[9] The work is related to the question of the physics of high-T_c-superconductors in the low field limit. In these systems, the magnetic field penetrates above the lower critical field, the system in well-defined flux-lines (FL) each carrying a flux quantum. These lines interact with the disorder in the material, have internal elasticity, and repulse each other. It is also related to the field-theoretical issues of interacting line-systems in general.[10] The physics of the problem is similar to that of the one-line case[11,12,3] but shows interesting twists if one tries to understand the problem in the light of individual, independent objects/lines. In particular, we are going to consider by numerical, *exact* min-cost flow optimization computations, the difference in energy between the TPRM problem, the single-line ground-state and the "first excited state".

This excited state results from adhering to a hierarchical picture, in which the first polymer is first optimized given a disorder configuration, and then the next one is added by applying a hard-core repulsion, by increasing sufficiently the energy of the bonds already taken up by the first line. The procedure gives us two energies to compare with the true TPRM ground state energy E_2: the single line ground-state energy doubled, $2E_1$, and the sum of the ground-state energy E_1 and the energy of the first excited state E_1' in the single line problem. The two energy differences, $E_2 - 2E_1$ and $E_2 - E_1 - E_1'$ define two interaction energies of the two polymers. In an earlier paper, Tang[5] studied the TPRM in hierarchical lattices and in two dimensions with binary disorder. His main conclusion was, for the physically relevant real-space case, that the probability for an interaction energy exactly equal to zero (with binary disorder) decayed much faster than expected, the exponent being $-2/3$ instead of the $-1/3$ expected based on single-DP geometric arguments. We study both the interaction energies discussed above. We also comment on the topology of the TPRM ground-state. One of the main conclusions of our paper is that the TPRM ground-state is *nonseparable* at least in the particular geometry we use: the lines start next to each other but have arbitrary endpoints. This means that the optimization of the TPRM ground-state cannot be done in two quasi-independent steps by adding a second line to the first line in the one-line ground state without deforming the first line.

In addition to our choice for an ensemble for the TPRM system, there are at least two others. First, one may allow the polymers to start and exit the system in the longitudinal direction at arbitrary positions (with or without imposed periodicity). In this limit, once the system size H transverse to the polymer fluctuations is much larger than the geometric single-line w, $H \gg w$ can consider the two lines to reside in independent valleys of the energy landscape. Then, the interaction energy

results from extremal statistics and the joint optimization is semi-trivial.[13] The second choice is to choose H constant, let the line length L vary, and study the problem in the presence of translational invariance, as a function of H. The latter one would be more closely related to a "true" TPRM problem, but it is on the other hand easy to see that in the thermodynamic limit, it is difficult to insert a second line (the excited state) into the system due to the mutual hard-core exclusion.

The structure of the paper is as follows. In Sec. 2, we formulate the problem and outline the relevant scaling exponents to be studied later. Section 3 discusses the numerical method, which is computationally much faster than the transfer matrix method when the latter is applied *correctly* to the two polymer problem. We show that the problem is NOT separable, so, there is no way in which the problem can be dealt with recursively and thus no way in which the transfer matrix method can be applied efficiently. In Sec. 4, we give the numerical data concerning the scaling behavior. Finally, Sec. 5 finishes the paper with conclusions.

2. Two Directed Polymers in a Random Medium

The continuum Hamiltonian for the TPRM problem is written in all generality as:

$$H = H_{\text{elastic}}\{x_1(t), x_2(t)\} + H_{\text{random}}\{x_1(t), x_2(t)\} + H_{\text{interaction}}\{x_1(t), x_2(t)\}\,, \quad (1)$$

where the configuration of the two lines is defined by the two coordinates $x_1(t)$ and $x_2(t)$, parameterized by the variable t. For *directed* polymers, t can identified with the longitudinal coordinate in d-dimensional space and $x_{1,2}$ with the $d-1$ transverse coordinates. The first term H_{elastic} describes the elastic energy of the lines being quadratic in the derivatives and the second $H_{\text{random}}\{x_1(t), x_2(t)\} = \int_0^{t_{\max}} dt\{V_r(x_1(t)) + V_r(x_2(t))\}$ the interaction with the quenched random potential being the same for both lines. Here, we consider uncorrelated point disorder, i.e., we have $\langle V_r(x)V_r(x')\rangle \propto \delta^d(x-x')$.

The last term $H_{\text{interaction}}\{x_1(t), x_2(t)\} = \int_0^{t_{\max}} dt V_{\text{int}}(x_1(t) - x_2(t))$ is the interaction energy between the two lines and gives rise to a variety of phenomena. First, for ground-state problems, the case of an attractive potential or zero potential is obviously trivial: the two lines will localize to the same ground-state. In this paper, we are going to deal with a hard-core repulsion between lines 1 and 2. This implies a delta-function-like $V_{\text{int}} \sim V_0\delta^d(x_1 - x_2)$ with $V_0 \to \infty$ so that overlap between the lines is strictly excluded. Would one allow for e.g., a finite V_0, then, the one-line ground-state would act as a pinning defect and the physics would slowly cross-over from the hard-core case to that of two lines with soft-core repulsion as V_0 is decreased.

The simplest scaling picture for the TPRM in the presence of a hard-core interaction V_{int} consists of two independent directed polymers, one being in the one-line global minimum and the second being in the first local minimum or the first excited state. This picture implies that the TPRM ground-state would be *separable* that is it could be constructed by a successive optimization procedure. This turns out to

be *false*, but the construction gives a definition for the effective interaction energy

$$V_{\mathrm{int,eff}} = E_1 + E_1' - E_2 \propto L^{\theta_V} \,, \tag{2}$$

where E_1 refers to the single-DP ground-state energy in a particular sample, E_1' to the first excited state, and E_2 is the true TPRM ground-state energy. θ_V defines a scaling exponent for this particular form of interaction energy. Recall that one has $E_1 \simeq AL + \bar{A}L^{\theta_1} + \cdots$ and that the same is expected of E_1' as well where A, $\bar{A}$ are disorder and dimension-dependent nonuniversal pre-factors. For E_2, it is to be expected that the scaling is of the same form $E_2 \simeq BL + \bar{B}L^{\theta_2}$ where the exponent θ_2 measures the energy fluctuations of the TPRM ground-state, $\Delta E_2 = \langle E_2^2 \rangle - \langle E_2 \rangle^2 \propto L^{\theta_2}$. The ensemble-averaged $V_{\mathrm{int,eff}}$ allows one to note that since the energy and its fluctuations have an upper bound, the separable trial ground-state θ_V should be limited from above by θ_1.

Likewise, the interaction energy can be described by the energy of the TPRM ground-state minus twice the single line energy, i.e.,

$$\delta E_2 = E_2 - 2E_1 \propto L^{\theta_E} \,. \tag{3}$$

Here, θ_E defines another scaling exponent characterizing the TRPM groundstate. One has naturally $\delta E_2 + V_{\mathrm{int,eff}} = E_1' - E_1 \geq 0$ and in particular if the single-line problem has two geometrically independent, energetically degenerate solutions then the sum is zero. Since δE_2 is positive semi-definite sample-to-sample, a lower limit for θ_2 is θ_1 and therefore by this dual construction, one would expect that $\theta_2 = \theta_1$. In this work, we do not consider the roughness properties of the two-line system but note that one would likewise expect that $\zeta_2 = \zeta_1$. Figure 2 shows examples from two and three dimensions of situations in which the true TPRM ground-state is *nonseparable*, i.e., it cannot be constructed out of the states with energies E_1 and E_1' and has thus a nonzero $V_{\mathrm{int,eff}}$. A closer look reveals that this is due to changes in the configurations of both the lines.

3. Numerical Method

Here, we define the lattice version of the continuum model of two random polymers with hard-core interactions in a random environment introduced in the preceding section. The polymer configuration will live on the *bonds* of a square lattice, each bond can only be occupied by a segment of a single polymer (hard-core interactions) and the occupation of each bond (ij) costs a particular amount of energy e_{ij}. This models the random part H_{random} of the continuum Hamiltonian, Eq. (1), but also the elastic part H_{elastic}, since all bonds cost some positive energy such that in case of no disorder straight lines are the minimum energy configurations. In such a way, we formulate the lattice model that the connection to a minimum cost flow problem becomes obvious.[14] Consider the energy function

$$H(\mathbf{z}) = \sum_{(ij)} e_{ij} \cdot z_{ij} \,, \tag{4}$$

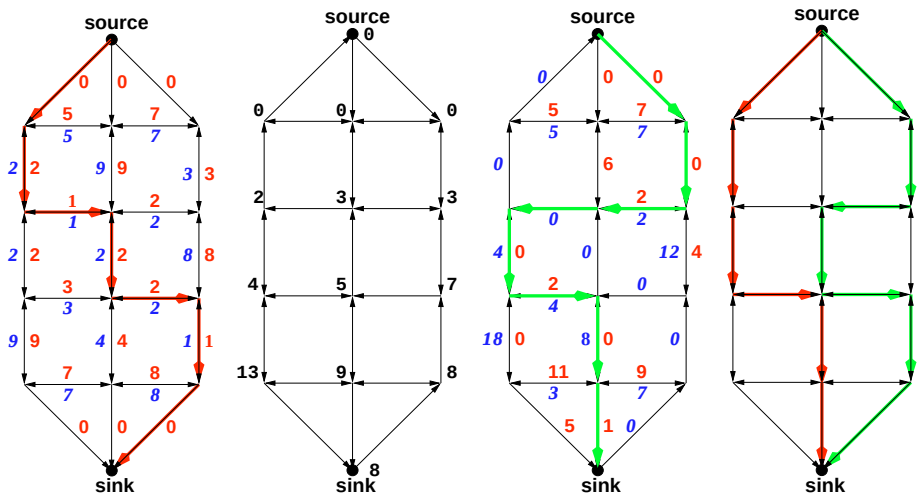

(a) (b) (c) (d)

Fig. 1. Sketch of the successive shortest path algorithm for the solution of the minimum cost flow problem described in the text. (a) Network for $N = 0$, the numbers are the bond energies (or costs) e_{ij}. If the flow is nonzero, a counter-flow will reduce the cost of the bond and thus, there are two costs associated to each direction. The dark thick line is a shortest path from source s to sink t. (b) The residual network G_c^0 for a flow as in (a) with the update node potentials. (c) G_c^0 from (c) with the updated reduced costs plus the shortest path from s to t in G_c^0 indicated by the bright thick line. (d) Optimal flow configuration for $N = 2$ in the original network. Note that the 2-line state is *not separable*, i.e., it does *not* consist in the line of (a) plus a 2nd line.

where $\sum_{(ij)}$ is a sum over all *bonds* (ij) joining site i and j of a d-dimensional lattice, e.g., a rectangular $(L^{d-1} \times H)$ lattice, with periodic boundary conditions (b.c.) in $d-1$ space direction and free b.c. in one direction. The bond energies $e_{ij} \geq 0$ are quenched random variables that indicate how much energy it costs to put a segment of a polymer on a specific bond (ij). For convenience, we consider forward and backward arcs such that for each pair of sites i, j, there is a bond (ij) *and* a bond (ji). Initially, the costs for bond (ij) and (ji) are the same, but in the residual graph, after the first line has been added, this is not true any more. The variables describing the two polymers are $z_{ij} \in \{0, 1\}$ (for hard-core interactions), $z_{ij} = 1$ if a FL runs from site i to j, $z_{ij} = 0$ otherwise. For the configuration to form *lines* on each site of the lattice, all incoming flow should balance the outgoing flow, i.e., the flow is divergence free, which means that

$$\forall i\colon (\nabla \cdot \mathbf{z}) := \sum_{j \text{ n.n. of } i} z_{ji} - \sum_{j \text{ n.n. of } i} z_{ij} = 0\,. \tag{5}$$

Obviously, the polymer has to enter, and to leave, the system somewhere. We attach two neighboring sites of one free boundary to an extra site (via energetically neutral arcs, $e = 0$), which we call the source s, and the other side to another extra site, the target, t as indicated in Fig. 1(a). Now, one can push one line through the system

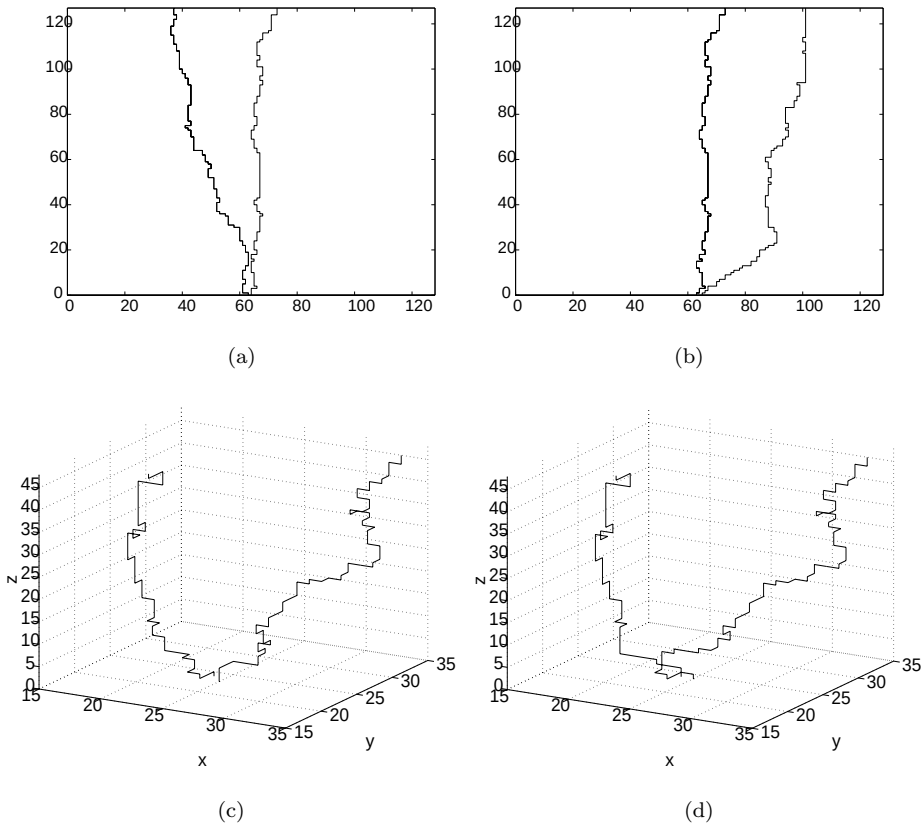

Fig. 2. (a) Two-polymer ground-state in 2D, (b) the same system but with the first (1-line GS) frozen first. The energy of the configuration in (a) is lower. Note that in (a), the 1-line GS is the left line of (b). The fact that in (a), the 1-line GS is minimally deformed (in the lower part in order to give the 2nd line a bit of space where energetically favorable) produces a 2-line GS that is totally different (concerning the 2nd line) from the configuration in (b). (c) The TPRM GS in 3D, (d) as (b) but in 3D. In both the 2D and the 3D comparisons, the disorder landscape is the same.

by inferring that s has a source strength of $+1$ and that t has a sink strength of -1, i.e.,

$$(\nabla \cdot \mathbf{z})_s = +N \quad \text{and} \quad (\nabla \cdot \mathbf{z})_t = -N\,, \tag{6}$$

with $N = 1$. Thus, the 1-line problem consists in minimizing the energy in Eq. (4) by finding a flow $\mathbf{z}$ in the network (the lattice plus the two extra sites s and t) fulfilling the constraints of Eqs. (5) and (6). Naively, one would expect that the 2-line problem consists simply in adding a second line to the 1-line configuration, avoiding the bonds already occupied due to the hard-core interaction we consider here. A glance at Fig. 1 convinces us that this is not correct and actually the main issue of the present paper is to provide evidence that the correct solution of the TPRM problem is significantly different from what one gets when assuming the

separability of the ground state. The algorithm by which one solves the TPRM problem is a standard application of min-cost flows to elastic line problems[14–16] but its detailed description sheds some light into why the GS is not separable.

The first key ingredient to treat the two-line problem (and the N-line problem in general[14]) is that one does not work with the original network. One considers the residual network $G_c(\mathbf{z})$ corresponding to the actual polymer configuration $\mathbf{z}$, which contains also the information about possibilities to send flow backwards (now with energy $-e_{ij}$ since one wins energy by reducing z_{ij}), i.e., to modify the actual flow. Suppose that we put one polymer along a shortest (smallest energy) path $P(s,t)$ from s to t, which means that we set $z_{ij} = 1$ for all arcs on the path $P(s,t)$. Then, the residual network is obtained by reversing all arcs and inverting all energies along this path, indicating that here we cannot put any further flow in the forward direction (since we assume hard-core interaction, i.e., $z_{ij} \leq 1$), but can send flow backwards by reducing z_{ij} on the forward arcs by one unit. This procedure is sketched in Fig. 1. Note that now the energy cost of a bond is not symmetrical ((ij) versus (ji)).

The second key ingredient is the introduction of a so called *node potential* $\boldsymbol{\varphi}$ that fulfills the relation

$$\varphi(j) \leq \varphi(i) + e_{ij} \tag{7}$$

for all arcs (ij) in the residual network, indicating how much energy $\varphi(j)$ it would *at least* take to send one unit of flow from s to site j, IF it would cost an energy $\varphi(i)$ to send it to site i. Obviously, $\boldsymbol{\varphi}$ is not uniquely defined via Eq. (7), for instance, $\varphi(i) = 0$ (for all i) is a node potential that is often used to initialize the algorithm discussed below. With the help of these potentials, one defines the reduced costs

$$c_{ij} = e_{ij} + \varphi(i) - \varphi(j) \geq 0\,. \tag{8}$$

The last inequality, which follows from the properties of the potential $\boldsymbol{\varphi}$ in Eq. (7) actually ensures that there is no loop $\mathcal{L}$ in the current residual network (corresponding to a flow $\mathbf{z}$) with negative total energy, since $\sum_{(ij)\in\mathcal{L}} e_{ij} = \sum_{(ij)\in\mathcal{L}} c_{ij}$, implying that the flow $\mathbf{z}$ is optimal.[15]

The idea of the *successive shortest path algorithm* is to start with an empty network, i.e., $\mathbf{z}^0 = 0$, which is certainly an optimal flow for $N = 0$, and set $\boldsymbol{\varphi} = 0$, $c_{ij} = e_{ij}$. One now successively adds lines to the system using the following iteration: suppose we have an optimal $(N-1)$-line configuration corresponding to the flow $\mathbf{z}^{N-1}$. The current potential is $\boldsymbol{\varphi}^{N-1}$, the reduced costs are $c_{ij}^{N-1} = e_{ij} + \varphi^{N-1}(i) - \varphi^{N-1}(j)$ and we consider the residual network G_c^{N-1} corresponding to the flow $\mathbf{z}^{N-1}$ with the reduced costs $c_{ij}^{N-1} \geq 0$. The iteration leading to an optimal N-line configuration z_{ij}^N is:

(1) Determine shortest distances $d(i)$ from s to all other nodes i with respect to the reduced costs c_{ij}^{N-1} in the residual network G_c^{N-1}.
(2) For all nodes i, update the potential: $\varphi^N(i) = \varphi^{N-1}(i) + d(i) - d(t)$.

(3) Let $P(s,t)$ denote a shortest path from node s to t. To obtain z_{ij}^N, increase (decrease) by one unit the flow variables z_{ij}^{N-1} on all forward (backward) arcs (ij) along $P(s,t)$ (see Fig. 1).

Note that due to the fact that the numbers $d(i)$ are shortest distances one has again $c_{ij}^N \geq 0$, i.e., the flow $\mathbf{z}^N$ is indeed optimal. To estimate the complexity of this algorithm, it is important to note that it is not necessary to determine shortest paths from s to *all* other nodes in the network; a shortest path from s to t is sufficient if one updates the potentials in a slightly different way.[15] Thus, the complexity of each iteration is the same as that of Dijkstra's algorithm for finding shortest paths in a network, which is $\mathcal{O}(M^2)$ for a naive implementation (M is the number of nodes in the network). We find, however, for the cases we consider (d-dimensional lattices), it roughly scales linearly in $M = L^d$. Thus, for N polymers, the complexity of this algorithm is $\mathcal{O}(NL^d)$.

In Fig. 2, we show the true ground state configuration for a specific disorder configuration in 2D and in 3D and compare it with the one-line ground state plus the first excited state (the latter defined as the ground state in the network that is left when the bonds occupied by the one-line ground state are excluded). This is a typical example in which the two-line configurations in 2D and 3D are distinct.

4. Results

For the actual computations reported in the following, we set the height of the system H equal to its lateral size L, i.e., $H = L$, yielding a square geometry in 2D and a cubic one in 3D and considered system sizes from $L = 16$ to $L = 256$ in 2D and from $L = 8$ to $L = 64$ in 3D. For each system size, the results are averaged over $N = 12\,000$ (2D) and $N = 8000$ (3D) disorder configurations, and quantities like E_1, E_2, δE_2, $V_{\mathrm{int,eff}}$ denote disorder averages from now on. As discussed in the previous section, the lines are forced by the boundary condition to start at neighboring sites. This is the "worst-possible" boundary condition, since obviously the interaction cost will be the highest (see the Introduction for a discussion).

We expect the various exponents that we estimate to be independent of the actual disorder we put in (as long as it is uncorrelated and does not have algebraic tails), nevertheless, we took two different probability distributions for the bond energies: (1) a *uniform* distribution for which $P(e_{ij}) = 1$ for $e_{ij} \in [0,1]$ and 0 otherwise; (2) a *binary* distribution in which e_{ij} is 1 with probability p and 0 with probability $1 - p$.

4.1. *Two dimensions*

Figure 3 shows the scaling of the two-line system energy and energy fluctuations for both a uniform distribution for the e_{ij}'s and a binary one with $p = 0.8$. As expected, the scaling of the total energy E_2 is linear and the fluctuations ΔE_2 scale with an exponent θ_2 with $\theta_2 \simeq \theta_1$, the one-line energy fluctuation exponent. This

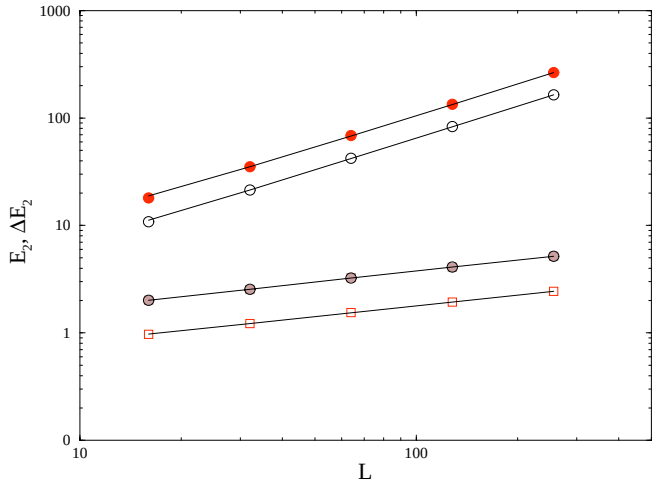

Fig. 3. Energy E_2 (black and white circles) and energy fluctuations ΔE_2 (grey circles and white squares) of the TPRM problem in two dimensions in a log–log plot. We show data for binary disorder ($e_{ij} \in \{0, 1\}$) (filled symbols) and the uniform distribution of e_{ij}'s (open symbols). One expects $E_2 \propto L$ and $\Delta E_2 \propto L^{\theta} = L^{1/3}$, correspondingly the straight lines have slopes 1 (top) and 1/3 (bottom).

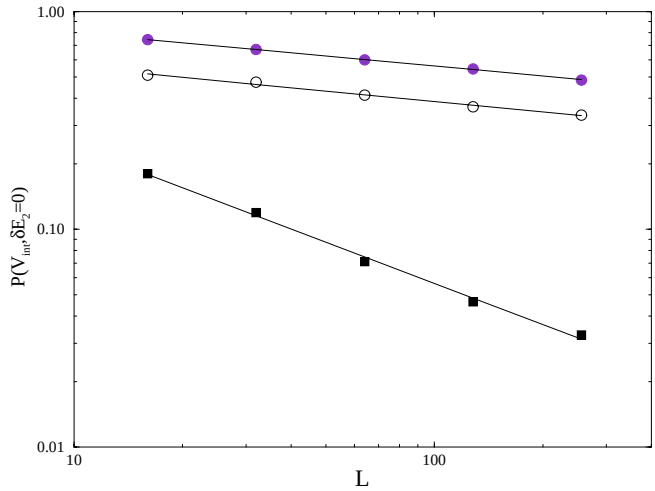

Fig. 4. $P(\delta E_2 = 0)$ (squares) and $P(V_{\text{int,eff}}) = 0$ (circles) versus L in 2D in a log–log plot. Data for both binary (filled symbols) and uniform (open symbols) distribution of the bond energies e_{ij}. The data follow the relations $P(\delta E_2 = 0) \propto L^{-a_1}$ and $P(V_{\text{int,eff}} = 0) \propto L^{-a_2}$ with a_1 and a_2 given by the slopes of the straight lines: $a_1 = 0.63 (\approx 1 - \theta)$ and $a_2 = 0.15$.

adheres to the picture that the energetics of the DP problem are in general dictated by the one-line exponent.

In Fig. 4, we show the probability that $\delta E_2 = 0$ as a function of system size. This measures the true degeneracy of the two-line system as the joint ground-state

can be obtained from two independent minima with the same energy. $P(\delta E_2 = 0) \propto L^{-a_1}$ with $a_1 = 0.63 \pm 0.03$ which is compatible with $a_1 = 2/3$ adhering thus to Tang's result,[5] which indicated $a_1 = 1 - \theta_1$. One can compare this with the scaling of $P(V_{\mathrm{int,eff}} = 0)$, which scales with an exponent $a_2 = 0.15 \pm 0.02$ for both distributions ($P \propto L^{-a_2}$). For δE_2 to be zero, one can assume that the groundstate and the first excited state (E_1, E_1') configurations come from two, geometrically distinct "trees". Then, we are left with a picture which explains the frequency of separable ground-states (with $\delta E_2 = 0$) by a picture in which the two lines belong to two neighboring trees in the energy landscape. This means that one considers an inverted structure in which the two lines end up next to each other but belong to two different trees (starting from $x = L$) with the same energy. Meanwhile, the interaction energy in general shows increasing "entanglement" meaning that the TPRM groundstate is restructured in the optimization, with a corresponding probability for a separable GS that decays with an exponent $a_2 = 0.15$.

Figures 5 and 6 discuss further the scaling of the mean interaction energies δE_2 and $V_{\mathrm{int,eff}}$ for the both distributions. Fitting our data for δE_2 to a simple power law, we obtain an effective exponent $\theta_E = 0.39 \pm 0.03$ for the system sizes we have studied. This estimate is close to the single line energy fluctuation exponent $\theta = 1/3$, but not exactly equal (even within the error bars). We cannot rule out the possibility that for larger system sizes the θ_E exponent crosses over to the one-line exponent, but the accuracy of our data does not provide a serious hint about such a crossover. In the limit $L \to \infty$, a two-line state that is made up of two optimal single line configurations confined to either half of the system ($x < L/2$ and $x > L/2$) gives an upper bound to δE_2 that scales with the single line exponent θ_1, but such a state does not fulfill the requirement that we explicitly force the two

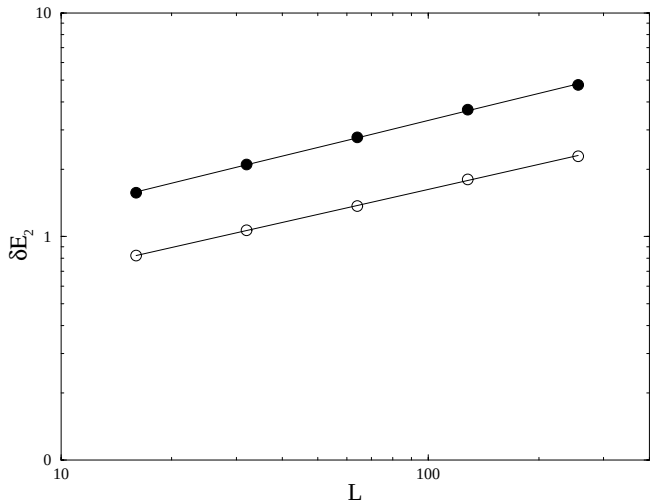

Fig. 5. δE_2 in 2D for binary (filled symbols) and uniform (open symbols) distribution of the bond energies e_{ij} in a log–log plot. It is $\delta E2 \propto L^{\theta_E}$ with $\theta_E = 0.39 \pm 0.03$.

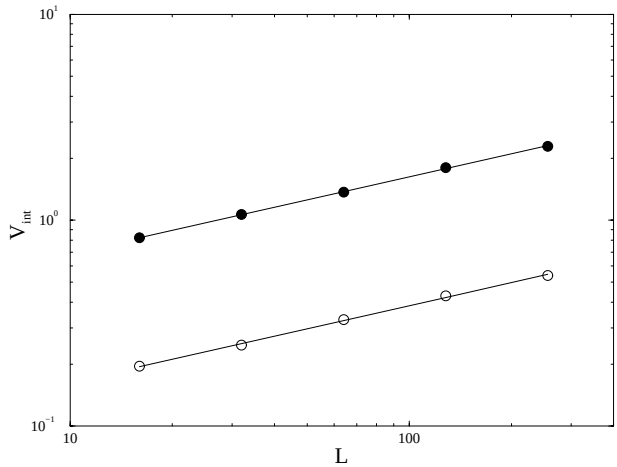

Fig. 6. $V_{\mathrm{int,eff}}$ in 2D for binary (filled symbols) and uniform (open symbols) distribution of the bond energies e_{ij} in a log–log plot. It is $V_{\mathrm{int,eff}} \propto L^{\theta_V}$ with $\theta_V = 0.39 \pm 0.03$.

lines to start close to each other. This interaction effect, which is not included in the single line scaling theory, leads to an enhancement of δE_2 and therefore to an increased effective exponent. Similarly, for $\theta_V = 0.39 \pm 0.03$, is found. In addition, as shown in Fig. 7, we can collapse the energy probability distributions for δE_2 and $V_{\mathrm{int,eff}}$ by using a two-exponent collapse. Note that this is different from the simple collapse one could attempt by using θ_E and θ_V. However, the two exponents combined make it so that the averages scale with θ_E and θ_V.

4.2. *Three dimensions*

Figure 8 shows the scaling of three-dimensional case again for both a uniform distribution for the e_{ij}'s and a binary one with $p = 0.8$ for the case of the two-line

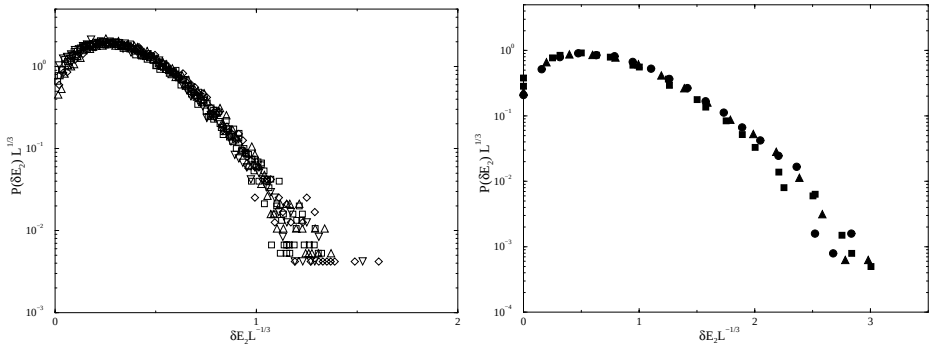

Fig. 7. Scaling plots of the probability distributions of δE_2 and $V_{\mathrm{int,eff}}$ in 2D for binary (filled symbols) and uniform (open symbols) distribution of the bond energies e_{ij} in a log–log plot.

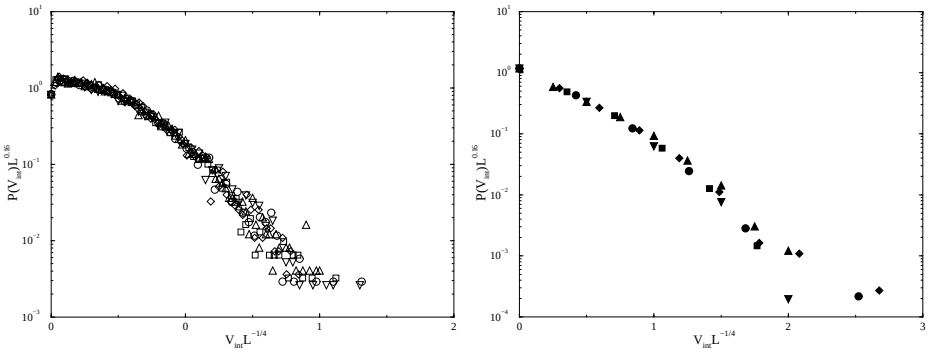

(c) (d)

Fig. 7. (*Continued*)

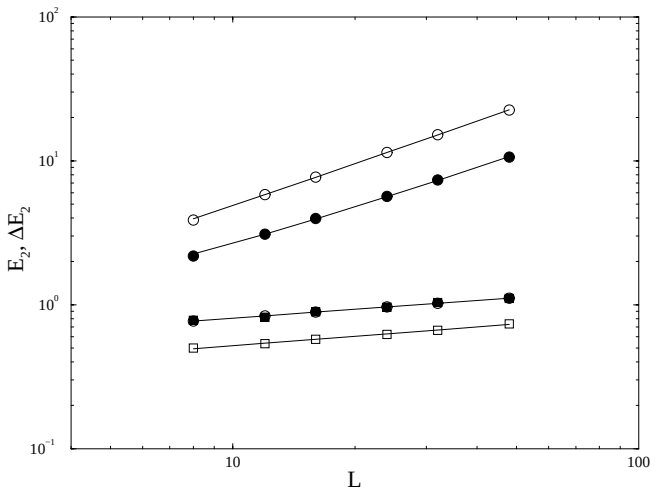

Fig. 8. Energy E_2 (circles) and energy fluctuations ΔE_2 (squares) of the TPRM problem in three dimensions in a log–log plot. We show data for binary disorder ($e_{ij} \in \{0, 1\}$) (filled symbols) and the uniform distribution of e_{ij}'s (open symbols). One expects $E_2 \propto L$ and $\Delta E_2 \propto L^{\theta}$, correspondingly the straight lines have slopes 1 (top) and 0.24 (bottom).

system energy and energy fluctuations. As expected, the scaling of the total energy E_2 is linear and the fluctuations ΔE_2 scale with an exponent θ_2 with $\theta_2 \approx \theta_1 \approx 0.24$, the one-line energy fluctuation exponent in three dimensions.

In Fig. 9, we show the probability that $\delta E_2 = 0$ as a function of system size. In 3D, for binary disorder, $P(\delta E_2 = 0) \propto L^{-a_1}$ with $a_1 \simeq 0.25 \simeq \theta_1$ in contrast with the geometric picture valid in 2D that would imply that $a_1 \simeq 0.75$. The scaling of $P(V_{\mathrm{int,eff}} = 0)$ cannot be described with a clear-cut universal exponent. We find $a_2 = 0.11 \pm 0.01$ for binary, and $a_2 = 0.05 \pm 0.01$ for continuous disorder ($P \propto L^{-a_2}$). Due to the fact that the decrease in $P(V_{\mathrm{int,eff}} = 0)$ is small for

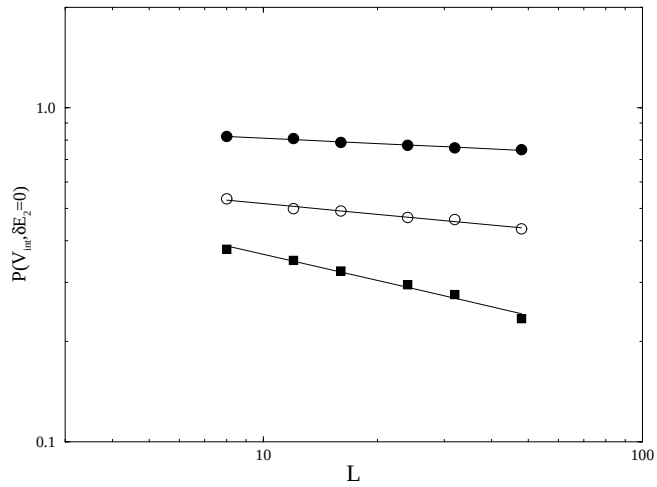

Fig. 9. $P(\delta E_2 = 0)$ (squares) and $P(V_{\mathrm{int,eff}}) = 0$ (circles) versus L in 3D in a log–log plot. Data for both binary (filled symbols) and uniform (open symbols) distribution of the bond energies e_{ij}. The data follow the relations $P(\delta E_2 = 0) \propto L^{-a_1}$ and $P(V_{\mathrm{int,eff}}) = 0 \propto L^{-a_2}$ with a_1 and a_2 given by the slopes of the straight lines: $a_1 = 0.25$ and $a_2 = 0.11$, 0.05 for binary and continuous disorder, respectively.

the range of system sizes considered, this does not exclude that the value of the exponent a_2 has a general, small value $a_2 \simeq 0.1$. The value of a_2 is trivially bounded from above by a_1, which is in agreement with the observations.

Again, the interaction energy in general shows increasing entanglement with a probability for a separable GS that decays with novel exponents a_1, a_2. The result

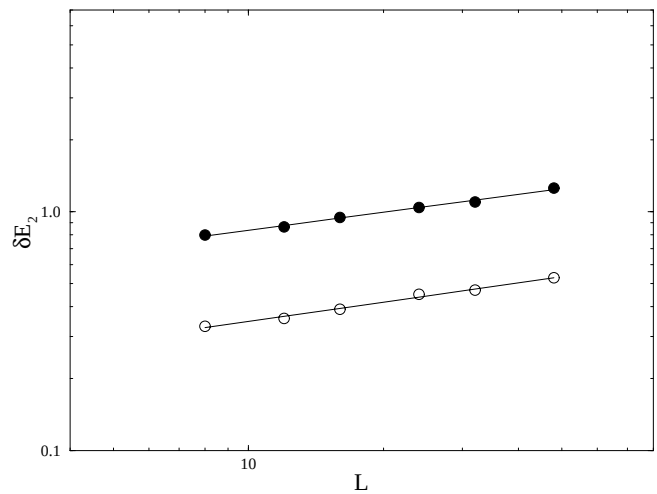

Fig. 10. δE_2 in 3D for binary (filled symbols) and uniform (open symbols) distribution of the bond energies e_{ij} in a log–log plot. It is $\delta E_2 \propto L^{\theta_E}$ with $\theta_E = 0.26 \pm 0.02$.

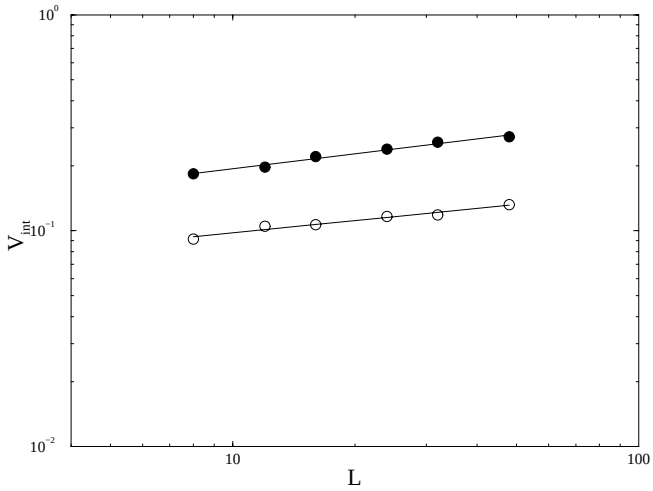

Fig. 11. $V_{\mathrm{int,eff}}$ in 3D for binary (filled symbols) and uniform (open symbols) distribution of the bond energies e_{ij} in a log–log plot. It is $V_{\mathrm{int,eff}} \propto L^{\theta_V}$ with $\theta_V = 0.21 \pm 0.02$.

that $a_1 \neq 1 - \theta_1$ in 3D can be attributed to the lack of hard-core expulsion. This means that one can now consider two paths "inside the same valley" (i.e., the transverse distance of the paths is not affected by the hard-core repulsion). The question how often two lines can have a degenerate energy, $E_1 = E_1'$, is thus answered indirectly by our scaling result for the exponent a_1. The physical implication is that in 3D, it is relatively easier for two lines to have the same energy, compared to 2D. Like in 2D, we are left without an effective argument for the exponent a_2. Here, matters are further complicated by the fact that the two exponents for respective disorders are slightly different, and the effective value is very small.

Figures 10 and 11 further discuss the scaling of the mean interaction energies δE_2 and $V_{\mathrm{int,eff}}$ for the continuous distributions. The 3D exponents become $\theta_E = 0.26 \pm 0.02$ and $\theta_V = 0.21 \pm 0.02$. Now, in particular, θ_V is closer to θ_1 than in the 2D case. As shown in Fig. 12, we can collapse the energy probability distributions for δE_2 and $V_{\mathrm{int,eff}}$ by using, as in 2D, a two-exponent collapse. For binary disorder, the collapse of the data makes sense in both cases, for continuous, we restrict ourselves to δE_2.

5. Conclusions

In this paper, we have investigated the joint ground-state of two directed polymers in a random medium, the TPRM problem. The main questions addressed here are whether the scaling of the TPRM can be described with the one-line exponents and an associated picture of behavior and if not, when. To this effect, we define here the interaction energy $V_{\mathrm{int,eff}}$ which measures the energy difference to a separable groundstate, i.e., a state that can be constructed successively out of the one-line groundstate and the one-line excited state excluding the groundstate.

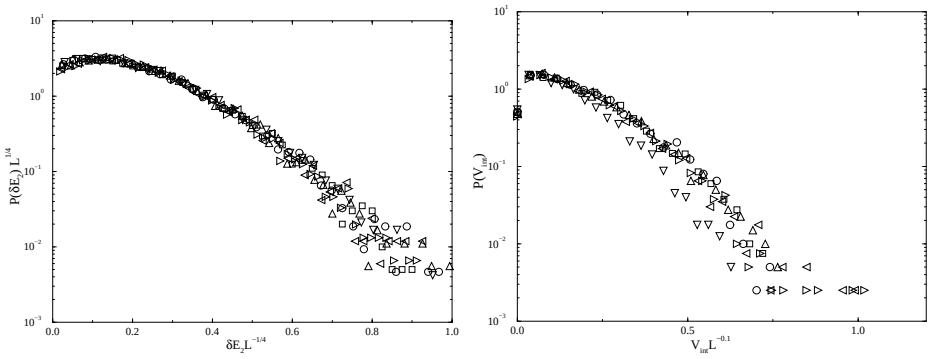

(a) (b)

Fig. 12. Scaling plots of the probability distributions of δE_2 and $V_{\mathrm{int,eff}}$ in 3D for the uniform distribution of the bond energies e_{ij} in a log–log plot.

Unsurprisingly, it turns out that $V_{\mathrm{int,eff}}$ as defined here seems to result in an *independent* exponent that cannot be explained by the one-line scaling arguments, if one considers the probability of a separable groundstate in which $V_{\mathrm{int,eff}}$ can be constructed trivially using two one-line state energies. This is natural since the probability measures the difference of the true TPRM ground-state to the "Ansatz" of two separable states and is thus the first nonanalytic and nontrivial correction characterizing the unique nature of the TPRM problem. This should generalize to situations with more than two lines in a natural fashion. The numerical value(s) for the interaction energy exponents θ_E, θ_V are in the vicinity of the energy fluctuation exponent, θ_1 in both 2D and 3D. On physical grounds, one would expect that the exponents are limited from below by θ, and this agrees with our estimates in all the cases. Our numerical data cannot exclude the case that these exponents are in fact equal to θ_1. In 2D, an upper bound for E_2 is given by the energy increase of a DP starting next to a self-affine wall, which problem to our knowledge has not been studied in this context. In 3D, the situation is more difficult since the lines can pass (wind around) each other. This is reflected in some of the features of the TPRM energetics, like the degeneracy of δE_2, which is clearly related to the single-line picture in two dimensions. In three dimensions, this is no longer true due to the lack of excluded volume effects (like in 2D). We lack a geometrical explanation for the scaling of the degeneracy exponent a_1 in this higher-dimensional case.

Finally, we would like to point out some directions for further studies. In this work, we have restricted ourselves to the "wedge boundary condition". That is, the two DP's of the TPRM problem are forced to start next to each other. There are two other scaling limits worth a study. Varying the start- and endpoints/boundary conditions would make it possible to study the competition of independent valley effects to internal reorganization — like here — inside the same valley. In the former case, the statistics of the energetics are expected to follow from rare event

statistics,[13] and since the DP's search for the two lowest energy minima in the landscape $V_{\mathrm{int,eff}} = 0$ (the GS is separable) while δE_2 follows from extremal statistics since it is the difference between two extremal variables. The second possibility for the scaling limit, is to use free boundary conditions for the ends but study systems with periodic boundary conditions or hard walls in the transverse direction. In the former case, one could investigate the center-of-mass behavior, while the latter, one has a caveat mentioned in the introduction (the first excited state is severly restricted by the GS). Our work also implies that the scaling functions of the distributions of the interaction energy would merit further study.

Acknowledgments

This work has been financially supported by the Academy of Finland and the German Academic Exchange Service (DAAD) within a common exchange project, and separately, by the A. of F.'s Finnish Centre of Excellence Programme. V.P. would like to acknowledge the hospitality of University of Cologne.

References

1. T. Halpin-Healy and Y.-C. Zhang, *Phys. Rep.* **254**, 215 (1995).
2. M. Kardar, G. Parisi, and Y.-C. Zhang, *Phys. Rev. Lett.* **56**, 889 (1986).
3. M. Mezard, *J. Physique* **51**, 1831 (1990).
4. T. Nattermann, M. Feigel'man, and I. Lyuksyutov, *Z. Phys. B* **84**, 353 (1991).
5. L. H. Tang, *J. Stat. Phys.* **77**, 581 (1994).
6. S. Mukherji, *Phys. Rev. E* **50**, R2407 (1994).
7. H. Kinzelbach and M. Lässig, *Phys. Rev. Lett.* **75**, 2208 (1995).
8. T. Hwa and D. Fisher, *Phys. Rev. B* **49**, 3136 (1994).
9. Note that we do not explicitly exclude overhangs in the polymer configuration, which for *directed* polymers are excluded. For a single line, overhangs are irrelevant such that the universal selfsimilar properties of a polymer and directed polymer are identical. For two lines, the question of the relevance of overhangs has not been studied yet.
10. M. Lässig, *J. Phys. C* **10**, 9905 (1998).
11. M. Kardar, *Phys. Rev. Lett.* **55**, 2235 (1985); D. Huse and C. L. Henley, *Phys. Rev. Lett.* **54**, 2708 (1985); M. Kardar, *Phys. Rev. Lett.* **55**, 2923 (1985).
12. M. Kardar and Y.-C. Zhang, *Phys. Rev. Lett.* **58**, 2087 (1987); T. Nattermann and R. Lipowski, *Phys. Rev. Lett.* **61**, 2508 (1988); J. Derrida and H. Spohn, *J. Stat. Phys.* **51**, 817 (1988); G. Parisi, *J. Physique* **51**, 1695 (1990); D. Fisher and D. Huse, *Phys. Rev. B* **43**, 10728 (1991).
13. E. T. Seppälä, M. J. Alava, and P. M. Duxbury, *Phys. Rev. E* **63**, 66110 (2001); cond-mat/0102318.
14. H. Rieger, *Phys. Rev. Lett.* **81**, 4488 (1998).
15. H. Rieger, "Frustrated systems: ground state properties via combinatorial optimization," *Lecture Notes in Physics 501* (Springer-Verlag, Heidelberg, 1998); R. Ahuja, T. Magnanti, and J. Orlin, *Network Flows* (Prentice Hall, New Jersey, 1993).
16. M. Alava, P. Duxbury, C. Moukarzel, and H. Rieger, in *Phase Transitions and Critical Phenomena*, Vol. 18, eds. C. Domb and J. L. Lebowitz (Academic Press, Cambridge, 2001), pp. 141–317.